

## ARTICLE

## OPEN



# Dysregulated miR-124 mediates impaired social memory behavior caused by paternal early social isolation

Sijia Chen<sup>1,2,6</sup>, Shixin Ding<sup>1,2,6</sup>, Yingting Pang<sup>1,3</sup>, Yuxi Jin<sup>1,2</sup>, Peng Sun<sup>1,2</sup>, Yue Li<sup>1,2</sup>, Min Cao<sup>1,2</sup>, Yimiao Wang<sup>1,2</sup>, Ze Wang<sup>1,3</sup>, Tianqi Wang<sup>1,3</sup>, Ying Zou<sup>1,3</sup>, Yanli Zhang<sup>1,4,5</sup>✉ and Ming Xiao<sup>1,2,3,4</sup>

© The Author(s) 2024

Early social isolation (SI) leads to various abnormalities in emotion and behavior during adulthood. However, the negative impact of SI on offspring remains unclear. This study has discovered that paternal early SI causes social memory deficits and anxiety-like behavior in F1 young adult mice, with alterations of myelin and synapses in the medial prefrontal cortex (mPFC). The 2-week SI in the F1 progeny exacerbates social memory impairment and hypomyelination in the mPFC. Furthermore, the down-regulation of miR-124, a key inhibitor of myelinogenesis, or over-expression of its target gene Nr4a1 in the mPFC of the F1 mice improves social interaction ability and enhances oligodendrocyte maturation and myelin formation. Mechanistically, elevated levels of miR-124 in the sperm of paternal SI mice are transmitted epigenetically to offspring, altering the expression levels of miR-124/Nr4a1/glucocorticoid receptors in mPFC oligodendrocytes. This, in turn, impedes the establishment of myelinogenesis-dependent social behavior. This study unveils a novel mechanism through which miR-124 mediates the intergenerational effects of early isolation stress, ultimately impairing the establishment of social behavior and neurodevelopment.

*Translational Psychiatry* (2024)14:392; <https://doi.org/10.1038/s41398-024-03109-1>

## INTRODUCTION

Harmonious and enriching interpersonal relationships contribute to physical and mental health [1, 2]. Adverse childhood experiences, such as social maltreatment and neglect, not only impact the establishment of behavior and neurodevelopment but also increase the risk of developing neuropsychiatric disorders [3]. Similarly, animal experiments have shown that early social isolation (SI) in rodents can lead to cognitive impairment, balance disorder, aggressive behavior, and social withdrawal in adulthood [4–6].

Furthermore, both maternal and paternal adverse childhood experiences can affect the emotional, behavioral, and mental health of their offspring [7, 8]. Retrospective data has confirmed that paternal depression increases risk of depression during adolescence [9, 10]. Children with parents suffering from post-traumatic stress disorder (PTSD) may exhibit a higher incidence of PTSD-like symptoms even without traumatic stress exposure [11]. Similarly, offspring with fathers experiencing chronic social defeat stress often exhibit depression- and anxiety-like behaviors [12]. However, the negative effects of paternal early SI on offspring behavior and neurodevelopment remains unknown.

Accumulated epigenetic evidence demonstrated that various types of stress can be transmitted from parents to offspring through multiple mechanisms including miRNAs, extracellular vesicles, DNA methylation, and histone modifications, thereby affecting the neurodevelopment and behavior of offspring [13–15]. Increased glucocorticoid exposure alters the miRNA expression profile in father's sperm and transmits anxiety- and

depression-like phenotypes to offspring [16]. Similarly, paternal adverse social experiences reprogram the hypothalamus-pituitary-adrenal (HPA) axis in the F1 generation, leading to an upregulation of corticosterone (Cort)-related gene expression levels in the hypothalamus and anxiety-like behavior [17, 18]. However, the potential mechanisms of behavior disorders in offspring with paternal early SI are not yet clear.

In this study, we subjected weaned male C57BL/6J mice to SI for 3 weeks and then bred them with aged-matched female mice to obtain F1 mice. We evaluated the social interaction, anxiety-like behavior, and short-term working memory of F1 young adult mice with or without 1- or 2-week SI exposure. We then investigated changes in myelin and synapse ultrastructure and related proteins in several key brain regions that regulate social behavior including the medial prefrontal cortex (mPFC), hippocampus, and amygdala [19, 20]. We also screened several miRNAs involved in social behaviors in the sperm of paternal SI mice, further confirmed their presence in the serum and mPFC of F1 offspring whose fathers were quarantined. We down-regulated miR-124, a key inhibitor of myelinogenesis [5] and overexpressed its target gene, nuclear receptor subfamily 4 group A member 1 (Nr4a1) [5], in the mPFC of the F1 mice from SI fathers, respectively, to observe their effects on myelin sheath and social behavior. Based on previous finding that miR-124 inhibits glucocorticoid receptor (GR) expression in oligodendrocytes (OLs) [21], we further investigated whether the HPA axis is involved in miR-124/Nr4a1 regulation of myelinogenesis in offspring with paternal SI.

<sup>1</sup>Jiangsu Key Laboratory of Neurodegeneration, Nanjing Medical University, Nanjing 211166, China. <sup>2</sup>Center for Global Health, Nanjing Medical University, Nanjing 211166, China.

<sup>3</sup>Brain Institute, Nanjing Brain Hospital, Nanjing Medical University, Nanjing 210029, China. <sup>4</sup>Changzhou Medical Center, Nanjing Medical University, Changzhou 213003, China.

<sup>5</sup>The Affiliated Changzhou Second People's Hospital of Nanjing Medical University, Changzhou Second People's Hospital, Changzhou 213000, China. <sup>6</sup>These authors contributed equally: Sijia Chen, Shixin Ding. ✉email: yanlizhang0229@njmu.edu.cn

Received: 2 January 2024 Revised: 19 September 2024 Accepted: 23 September 2024

Published online: 28 September 2024

## MATERIAL AND METHODS

### Animals and experimental design

C57BL/6J mice were purchased from Laboratory Animal Research of Nanjing Medical University. These mice were housed in a controlled environment with a constant temperature (18–22°C), regulated humidity (30–50%), a 12-hours light-dark cycle, and *ad libitum* access to food and water. All animal experiments were conducted in accordance with international standards for animal welfare and the guidelines of the Institute for Laboratory Animal Research of Nanjing Medical University (Approval No. IACUC: 2004013). Any relevant details of the animal protocol for this study have been approved by the Institute of Laboratory Animal Research of Nanjing Medical University.

As previously described in our earlier study [5], weaned male C57BL/6J mice were randomly divided into 2 groups: the group housing (GH) group, consisting of 5 mice per cage (31 cm × 22 cm × 15 cm), and the SI group, where one mouse was raised in a similar cage (Fig. 1A; Supplementary Fig. 1A). After 3-week rearing, the SI or GH group were randomly mated with age-matched and unexposed females, respectively. One male and one female newborn mice from each litter were selected and randomly assigned to one of the following groups: GH<sup>F0</sup>-GH<sup>F1</sup>, GH<sup>F0</sup>-SI<sup>F1</sup>, SI<sup>F0</sup>-GH<sup>F1</sup>, and SI<sup>F0</sup>-SI<sup>F1</sup> (Supplementary Table S1). If the offspring in few litters belonged to the same gender, only one mouse was selected. The experiments involving these F1 mice were conducted after 1- or 2-week corresponding rearing, respectively (Fig. 1A; Supplementary Fig. 1A).

### Behavior tests

**Three-chamber test.** The three-chamber test, comprising sociability and social novelty experiments, was performed to assess social interaction preference and social memory in mice [22]. The experimental setup consisted of 3 rectangular boxes (40 cm × 40 cm × 30 cm) separated by transparent plexiglass, with a channel in the middle connecting the 3 sections [23]. The test subject mouse was initially placed in the middle box for 5 minutes of free exploration before the sociability test. During the sociability test, an unfamiliar C57BL/6J mouse (Stranger-1) was placed in the metal cage (9 cm × 9 cm × 15 cm) on one side, while the cage on the other side remained empty. The subject mouse was then returned to the middle box and observed for 5 minutes. The social novelty experiment began to test 10 minutes afterwards, another unfamiliar C57BL/6J mouse (Stranger-2) was placed into the cage that was originally empty, the subject mouse was placed into the middle box and observed for another 5 minutes. The percentage of time spent in each box by the subject mouse was recorded and analyzed.

**Open-field test.** The open-field test utilized a square box (60 cm × 60 cm × 60 cm) to evaluate locomotion activity, exploratory behavior, and anxiety-like behavior in mice [24]. Each mouse was placed in the center of the area and allowed to explore freely for 5 minutes. The time spent and the number of entries into the center area, the defecation number and the traveling speed during the test were recorded and analyzed.

**Elevated plus maze (EPM).** The EPM test assesses the anxiety levels of animals by exploiting their fear of open environments and their inclination for exploring novel environments [25]. The maze consists of 2 opposite open arms and 2 opposite closed (wall covered) arms (10 cm × 50 cm). Test subject mice were placed in the center area and allowed to explore freely for 5 minutes. The percentage of time spent and the number of entries into the open arm were recorded and analyzed.

**Y-maze test.** The Y-maze test was employed to evaluate short-working memory in mice [26]. The maze consists of 3 identical arms, named the novel arm (NA), start arm (SA), and other arm (OA), respectively. In the first stage, the NA was blocked by a partition, and the test mouse was placed in the SA and freely explored the remaining maze for 5 minutes. Two hours later, the partition was removed, and the mouse was placed back in the SA to explore all 3 arms freely for 5 minutes. The percentage of time spent in and the number of entries into NA were recorded and analyzed.

**Primary cortical neurons culture.** Primary cortical neurons were isolated from 24-hour-old C57BL/6J neonatal mice. After removal of the meninges and blood vessels, the brain tissue was dissected into pieces and digested for 20 minutes in Dulbecco's Modified Eagle Medium (DMEM) medium (Gibco, #C11995500BT) with papain (30 U/mL, Sangon Biotech, #A003124-0100) and DNase I (2500 U, Sigma, #D4513) at 37°C. The cells were then

resuspended in neurobasal medium (Gibco, #21103049) supplemented with B27 supplements (2%, Gibco, #17504044) and Penicillin/Streptomycin (P/S) (1%, Gibco, #15140-122). The cells were seeded on poly-L-lysine (Sigma, #P6407)-coated 24-well (2.5 × 10<sup>5</sup> cells/well) or 6-well (1.5 × 10<sup>6</sup> cells/well) plates, with half of the medium being replaced every 2 ~ 3 day.

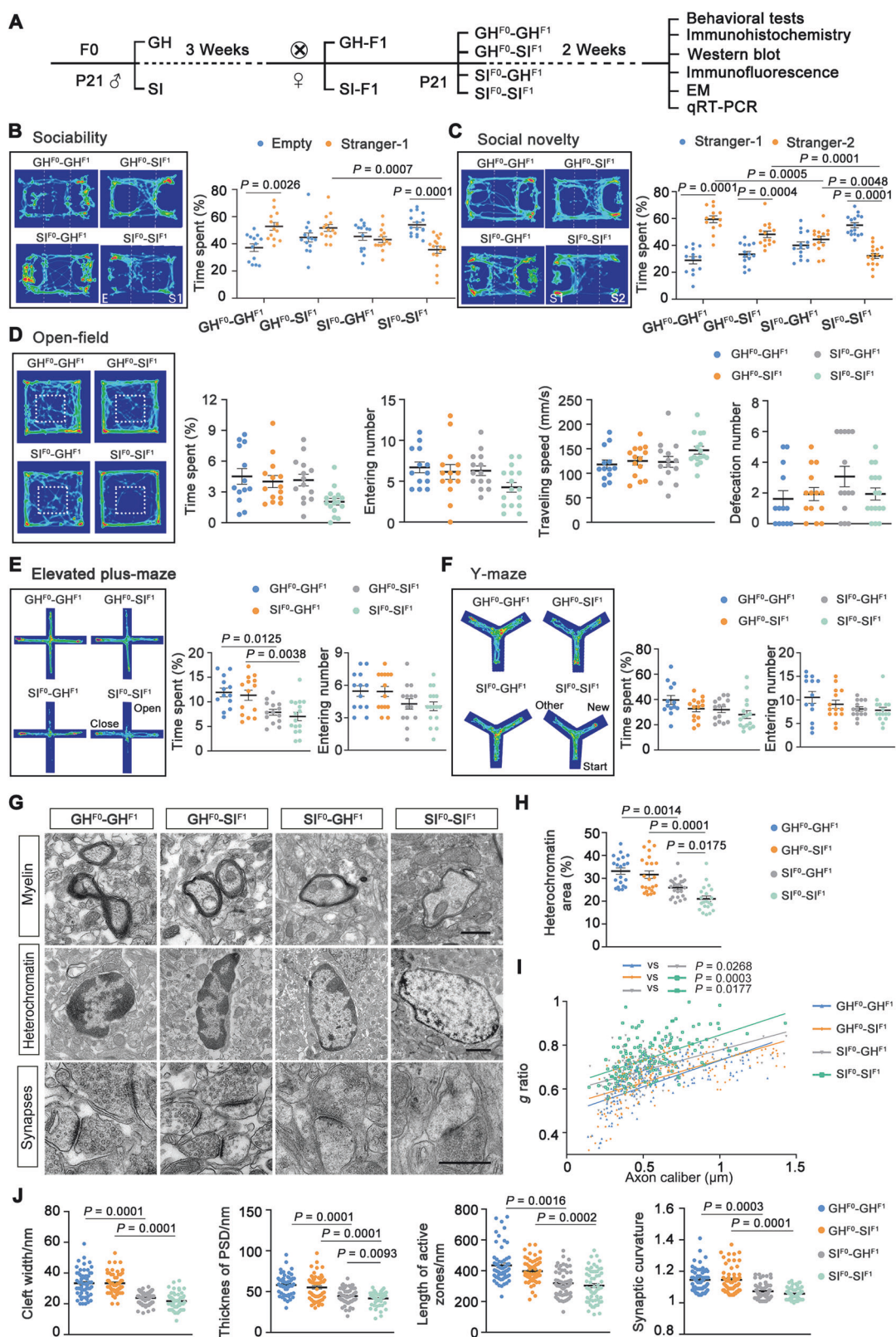
**Primary OL precursor cells (OPCs) culture and differentiation.** OPCs were isolated from postnatal 6-7-day-old C57BL/6J mice, following previously established protocols [5, 27, 28]. Briefly, after removing the meninges and blood vessels, the brain tissue was dissected into pieces and digested in DMEM medium at 37°C for 20 minutes with 30 U/mL papain and 2500 U DNase I. The cells were resuspended in phosphate-buffer saline (PBS) containing anti-O4 MicroBeads (Miltenyi Biotec, #130-094-543) and incubated at 4°C for 15 minutes. The beads were then captured by a column (Miltenyi Biotec, #130-042-201) to enrich the O4<sup>+</sup> OPCs. The cells were resuspended in DMEM-Nutrient Mixture F12 (F12) medium (Thermo Fisher, #11320-033) supplemented with 1% N2 (Thermo Fisher, #17502-048), 2% B27, 1% P/S and platelet derived growth factor-AA (40 ng/mL, R&D Systems, #1055-AA-050). The cells were then seeded on poly-L-lysine and laminin (Sigma, #114956-81-9) coated 24-well (2.5 × 10<sup>5</sup> cells/well) or 6-well (1.5 × 10<sup>6</sup> cells/well). The proliferation medium was replaced completely after 24 hours, and then half of the medium was replaced every 2 ~ 3 day. After 8 ~ 9 days, the cells were cultured in differentiation medium consisting of DMEM-F12 with 1% N2, 2% B27, 1% P/S, insulin (50 µg/mL, Sigma, #I-6634), triiodo tyrosine (40 ng/mL, Sigma, #T2877), and ciliary neurotrophic factor (1 ng/mL, R&D Systems, #557-NT) for differentiation.

**Cultured neurons and OLs treatment.** Cort treatment at a concentration of 10 nM was administered to cortical OLs and neurons for 48 hours, followed by the measurement of myelin length in OLs and dendrites length in neurons using immunofluorescence assays (24-well). Changes in the transcript levels of myelin- and synapse-related genes were analyzed by quantitative reverse transcriptase polymerase chain reaction (qRT-PCR) (6-well plates).

**Stereotaxic injection.** Mice under anesthesia were positioned in a stereotaxic apparatus with their skull surface exposed. AAV-U6-miR-124\_spG/AAV-CMV-Nr4a1 (2 µL, 1 × 10<sup>12</sup> v.g./mL) or control virus (AAV-CAG-EGFP/AAV-CMV-EGFP) (2 µL, 1 × 10<sup>12</sup> v.g./mL) was injected into the bilateral mPFC using a 33-gauge (Hamilton) syringe needle at the following coordinates: relative to bregma +1.5 mm anterior/posterior, −1.6 mm dorsal/benstral, and ± 0.3 mm medial/lateral at an infusion speed of 0.2 µL/minute [27]. Behavioral experiments were performed 2 weeks after virus injection. Following behavioral testing, the mice were sacrificed, and the brain sections were analyzed using EM, qRT-PCR, histology, or Western blot.

**Immunohistochemistry and immunofluorescence.** For immunohistochemistry, brain tissue sections were heated in a 95°C sodium citrate buffer solution for 15 minutes. Subsequently, the sections were incubated with 3% H<sub>2</sub>O<sub>2</sub> in PBS for 15 minutes and then blocked with 10% goat serum for 1 hour at room temperature. Primary antibodies, including anti-synaptophysin (SYP) (1:1000; Abcam, #ab32127), anti-NG2 (1:200; Millipore, #AB5320), anti-postsynaptic density protein 95 (PSD-95) (1:200; Abcam, #ab18258), and anti-myelin basic protein (MBP) (1:200; Abcam, #ab7349), were incubated overnight at 4°C. The next day, horseradish peroxidase-conjugated secondary antibodies (Vector laboratories, USA) and a DAB kit (Sigma-Aldrich, USA) were used for staining. For immunofluorescence, the sections were blocked with the 5% bovine serum albumin in PBS containing 0.3% Triton X-100 for 1 hour at room temperature. Subsequently, they were incubated with one or two of the following primary antibodies: anti-NG2 (1:200; Millipore, #AB5320), anti-NeuN (1:500; Abcam, #ab177487), anti-GR (1:200; CST, #12041S), anti-Nr4a1 (1:200; Novus, #NPB2-66980), anti-O4 (1:200; R&D, #MAB1326), anti-MBP (1:200; Abcam, #ab7349), anti-platelet derived growth factor receptor α (PDGFRα) (1:200; Abcam, #ab203491), anti-class III β-Tubulin (Tuj1) (1:200; SCBT, #sc-80005), anti-SYP (1:200), anti-PSD-95 (1:200), and anti-microtubule associated protein 2 (MAP2) (1:200; Millipore, #AB5622) antibody overnight at 4°C. Afterward, the sections were incubated with corresponding fluorescently labeled secondary antibodies (1:1000; Thermo Fisher, #A31571, #A31572, #A21206, #A21202, and #A31570) for 2 hours at 25°C. The nuclei were stained by DAPI staining solution (1:1000; Abcam, #ab228549) for 10 minutes at 25°C.

**Western blot.** Frozen mPFC, hippocampal and amygdala brain tissues were lysed in the RIPA buffer (Beyotime, #P0013B) with PMSF (Beyotime, #st506) and phosphatase inhibitors (Roche, #04906837001). Equal amounts



of protein (30 µg) were separated by 12% SDS-polyacrylamide gel electrophoresis and transferred on PVDF membranes. After blocking for 2 hours in 5% skim milk in TBST, the membranes were incubated at 4°C overnight with the primary antibodies of anti-SYP (1:10000; Abcam, #ab32127), anti-PSD-95 (1:1000; Abcam, #ab18258), anti-MBP (1:1000; Abcam, #ab7349), anti-NG2 (1:200; Millipore, #AB5320), or anti-GAPDH

(1:3000; Proteintech, #60004-1-Ig), and then with the horseradish peroxidase (HRP)-conjugated secondary antibodies (ZSGB-Bio, China) for 1 hour at room temperature. Bands were visualized using the ECL plus detection system (Imagequant LAS4000 mini, USA) and quantified by Image J 1.46R. Western blot uncropped data are presented in Supplementary Information.

**Fig. 1 Two-week isolation rearing in F1 mice exacerbates social memory and mPFC hypomyelination induced by paternal SI.** **A** Weaned mice were housed in group or isolation for 2 weeks for behavioral tests, followed by Western blot, immunohistochemistry, or immunofluorescence analysis. **B, C** Trajectory heat maps and statistical graph showing the percentage of time spent in each chamber during the three-chamber test ( $\text{GH}^{\text{F}0}\text{-}\text{GH}^{\text{F}1}$ :  $n = 13$ ;  $\text{GH}^{\text{F}0}\text{-}\text{SI}^{\text{F}1}$ :  $n = 14$ ;  $\text{SI}^{\text{F}0}\text{-}\text{GH}^{\text{F}1}$ :  $n = 14$ ;  $\text{SI}^{\text{F}0}\text{-}\text{SI}^{\text{F}1}$ :  $n = 16$ ). **D** Trajectory heat maps in the open-field test (left); the percentage of time spent, the number of entries into the center, total distances, and defecation number in the open field (right) ( $\text{GH}^{\text{F}0}\text{-}\text{GH}^{\text{F}1}$ :  $n = 13$ ;  $\text{GH}^{\text{F}0}\text{-}\text{SI}^{\text{F}1}$ :  $n = 14$ ;  $\text{SI}^{\text{F}0}\text{-}\text{GH}^{\text{F}1}$ :  $n = 14$ ;  $\text{SI}^{\text{F}0}\text{-}\text{SI}^{\text{F}1}$ :  $n = 16$ ). **E** Trajectory heat maps in the elevated plus maze (left); the percentage of time spent in and number of entries into the open arms (right) ( $\text{GH}^{\text{F}0}\text{-}\text{GH}^{\text{F}1}$ :  $n = 13$ ;  $\text{GH}^{\text{F}0}\text{-}\text{SI}^{\text{F}1}$ :  $n = 14$ ;  $\text{SI}^{\text{F}0}\text{-}\text{GH}^{\text{F}1}$ :  $n = 14$ ;  $\text{SI}^{\text{F}0}\text{-}\text{SI}^{\text{F}1}$ :  $n = 16$ ). **F** Trajectory heat maps in the Y-maze (left); The percentage of time spent in and number of entries into the NA of the maze (right) ( $\text{GH}^{\text{F}0}\text{-}\text{GH}^{\text{F}1}$ :  $n = 13$ ;  $\text{GH}^{\text{F}0}\text{-}\text{SI}^{\text{F}1}$ :  $n = 14$ ;  $\text{SI}^{\text{F}0}\text{-}\text{GH}^{\text{F}1}$ :  $n = 14$ ;  $\text{SI}^{\text{F}0}\text{-}\text{SI}^{\text{F}1}$ :  $n = 16$ ). **G** Representative EM images showing myelin (top), OLs nuclear heterochromatin (middle), and synaptic morphology (bottom) in the mPFC of mice from the different groups. Scale bars, 500 nm. **H** Graph showing the area percentage of OLs nuclear heterochromatin in  $\text{GH}^{\text{F}0}\text{-}\text{GH}^{\text{F}1}$  (21 nuclei),  $\text{GH}^{\text{F}0}\text{-}\text{SI}^{\text{F}1}$  (23 nuclei),  $\text{SI}^{\text{F}0}\text{-}\text{GH}^{\text{F}1}$  (24 nuclei), and  $\text{SI}^{\text{F}0}\text{-}\text{SI}^{\text{F}1}$  (21 nuclei) mice ( $n = 5$ ). **I** Scatter plot of  $g$  ratios with linear least squares fitting in  $\text{GH}^{\text{F}0}\text{-}\text{GH}^{\text{F}1}$  (170 axons),  $\text{GH}^{\text{F}0}\text{-}\text{SI}^{\text{F}1}$  (174 axons),  $\text{SI}^{\text{F}0}\text{-}\text{GH}^{\text{F}1}$  (163 axons), and  $\text{SI}^{\text{F}0}\text{-}\text{SI}^{\text{F}1}$  (165 axons) mice ( $n = 5$ ). **J** Graphs showing quantification of PSD, synaptic cleft width, length of the active zones, and synaptic curvature in  $\text{GH}^{\text{F}0}\text{-}\text{GH}^{\text{F}1}$  (59 synapses),  $\text{GH}^{\text{F}0}\text{-}\text{SI}^{\text{F}1}$  (58 synapses),  $\text{SI}^{\text{F}0}\text{-}\text{GH}^{\text{F}1}$  (60 synapses), and  $\text{SI}^{\text{F}0}\text{-}\text{SI}^{\text{F}1}$  (59 synapses) mice ( $n = 5$ ). Data are presented as mean  $\pm$  SEM and were analyzed by three-way ANOVA followed by Tukey's multiple comparisons test in **B, C**, and others were analyzed by two-way ANOVA followed by Tukey's post hoc test.

**qRT-PCR.** Total RNA was extracted from sperm, serum, mPFC, neurons, and OLs using TRIzol (Takara, #9109) according to the manufacturer's instruction. The qRT-PCR analysis of mRNA and miRNA expressions was performed on an ABI Step One Plus Real-Time PCR System (Applied Biosystems, Foster City, CA, USA) using the SYBR Green PCR master mix. The cDNAs were synthesized from 1  $\mu\text{g}$  total RNA using the Maxima First Strand Synthesis Kit (Takara, #RR047B) for qRT-PCR. qRT-PCR was performed by amplifying cDNA for 40 cycles using the SYBR Green PCR master mix. The amount of mRNA was normalized to GAPDH, and miRNA was normalized to U6. Primers (Supplementary Table S2, Tsingke Bio, China) were constructed based on the published nucleotide sequences. Relative quantification of target genes was analyzed using the  $2^{-\Delta\Delta\text{Ct}}$  method.

**Enzyme-linked immunosorbent assay (ELISA).** ELISA was employed to measure serum Cort concentration (R&D Systems, #KGE009). Mouse blood samples were kept overnight at 4°C and then centrifuged at 1 500 rpm for 20 minutes. The supernatant was carefully collected. HRP-conjugated reagent (100  $\mu\text{L}$ ) was added to both samples and standards, followed by incubation at 37°C for 60 minutes. Chromogen solution A (50  $\mu\text{L}$ ) and B (50  $\mu\text{L}$ ) were added and then incubated at 37°C for another 15 minutes. Then, the stop solution (50  $\mu\text{L}$ ) was added immediately. The density was examined at 450 nm within 15 minutes using a microplate reader (Thermo, #Varioskan LUX).

**Electron microscopy (EM).** EM detecting was performed to assess synaptic and myelin integrity. mPFC samples were stained with 0.5% uranyl acetate in 70% ethanol for 1 hour, followed by a series of ethanol dilutions, propylene oxide dehydration, embedding in Epon, and incubated at 60°C for 24 hours. The mPFC tissues in the Epon block were cut and sectioned, and ultrathin (70 nm) cross-sections were produced using an ultramicrosections (Leica EM UC7).

**Image analysis.** Images of immunohistochemistry and immunofluorescence were captured using a Leica DM4000 B microscope (Leica Microsystems, Wetzlar, Germany) and a Zeiss LSM 710 confocal microscope (Zeiss, Germany), respectively. Immunohistochemical staining of MBP, NG2, SYP, and PSD-95 were quantified by measuring the mean integrated optical density (MIOD) in the mPFC, hippocampus, and amygdala of mice. For immunofluorescence, more than 2 random images (400 $\times$ ) were selected for the region of interest (ROI) on each tissue slice. In addition, the counts of GR<sup>+</sup>, NeuN<sup>+</sup> GR<sup>+</sup>, NeuN<sup>+</sup> NG2<sup>+</sup>, NG2<sup>+</sup> GR<sup>+</sup>, and Nr4a1<sup>+</sup> O4<sup>+</sup> cells were reported as the number of positive cells per mm<sup>2</sup> in the mPFC. The positive area of MBP in the corresponding images was analyzed using ImageJ 1.53b (NIH, USA). Five or six mice per group were analyzed for all aforementioned indicators. Spearman's correlation index (at a significance level of 5%) was utilized to confirm the correlation of social behavior or EPM test with miR-124 and Nr4a1, respectively. The length of myelin branches of OLs and dendrites of neurons were measured using "Sholl" Analysis or "NeuroAnatomy" plugin in Image J 1.53b, respectively; with measurement started at a diameter of 0.05  $\mu\text{m}$  and proceeded with at 0.05  $\mu\text{m}$  intervals [5].

EM images were used to assess the integrity OLs and synaptic at an acceleration voltage of 120 kv using FEI Tecnai G2 electron microscope (FEI Company, USA). The presence of microtubules, absence of intermediate fibers, and glycogen particles were used to identify the extent of OLs heterochromatin. The total nuclear area of heterochromatin was calculated

by selecting it using the threshold tool, defined as a gray density of 100 or greater on 256 gray scales, and presented as a percentage of the total nuclear area. In addition, the  $g$  ratio, defined as the axon diameter divided by the diameter of the entire myelin fiber, was used to determine the degree of myelination, following established methods [29]. At least 20 myelinated axons were analyzed in each region of interest per mouse. Synaptic integrity was determined by measuring postsynaptic dense zone thickness, synaptic gap width, active zone length, and synaptic curvature. To avoid bias, image analysis was conducted by experimenters who were unaware of the experimental conditions. The image analysis software used was ImageJ 1.53b (NIH, USA).

### Statistical analysis

Statistical analysis was performed using GraphPad Prism 8.0.2 (GraphPad Software, USA). Two-tailed Student's  $t$  test was used for comparisons between 2 groups. For comparisons involving 3 or more groups, one-way ANOVA followed by Tukey's post hoc test, two-way ANOVA followed by Tukey's post hoc test or three-way ANOVA followed by Tukey's multiple comparisons test were employed. Unless otherwise specified, date was represented as mean  $\pm$  SEM with  $P < 0.05$  considered statistically significance. The main effects and interactions were reported in the supplement (Supplementary Excel 1).

## RESULTS

### Two-week isolation rearing in F1 mice exacerbates social memory impairment caused by paternal SI

Numerous studies have shown that parents' early life experiences not only influence the behavior and emotions of their offspring from their mothers, but also through their fathers [30, 31]. Therefore, we hypothesized that paternal behavioral and pathological damages caused by SI could be transmitted to the F1 generation. To test the hypothesis, we analyzed and compared behavioral and pathological changes among  $\text{GH}^{\text{F}0}\text{-}\text{GH}^{\text{F}1}$  mice,  $\text{GH}^{\text{F}0}\text{-}\text{SI}^{\text{F}1}$  mice,  $\text{SI}^{\text{F}0}\text{-}\text{GH}^{\text{F}1}$  mice, and  $\text{SI}^{\text{F}0}\text{-}\text{SI}^{\text{F}1}$  mice, as named in the experimental design section (Fig. 1A; Supplementary Fig. 1A). The three-chamber test revealed that paternal SI rearing impaired social memory abilities in offspring, as indicated by a decrease in time spent of stranger-2 chamber. F1 mice subjected to 2 weeks of SI exhibited worsened social memory impairments (Fig. 1B, C). In the 1-week SI group, the deterioration of the condition was not significant (Supplementary Fig. 1B, C).

In the EPM test, offspring mice whose fathers experienced early SI spent less time in the open arm compared to those whose fathers were raised in group housing; however, this phenomenon was not exacerbated by 1 or 2 weeks of SI stress (Fig. 1E; Supplementary Fig. 1E). Additionally, there were no significant changes in behavioral performance in Y-maze test and open field test among the four groups of mice (Fig. 1D, F; Supplementary Fig. 1D, F). In summary, the above data revealed social memory deficits and anxiety-like phenotypes in F1 adolescents with paternal SI, with 2 weeks of SI exposure further exacerbating their social memory disorder.

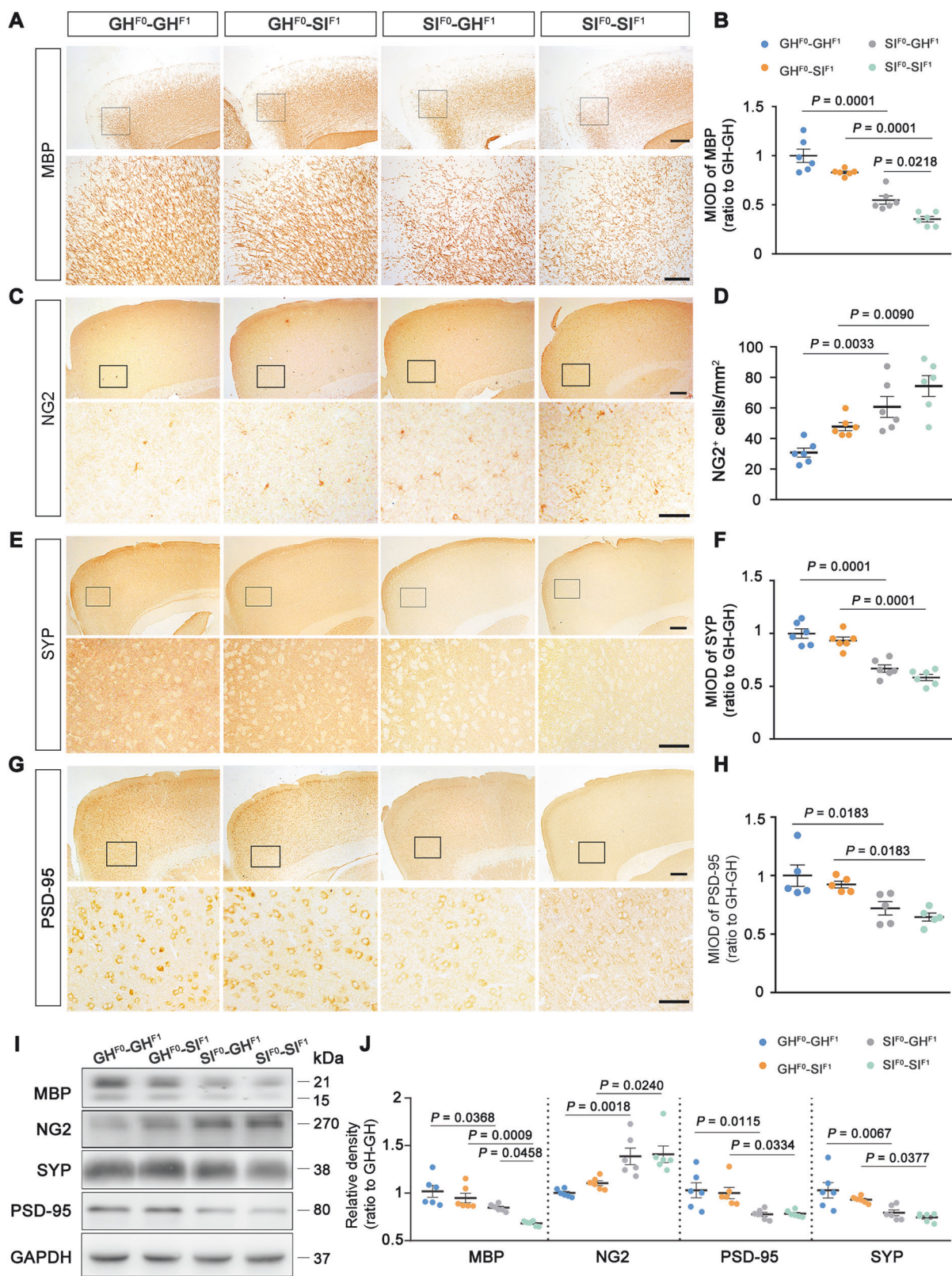


**Fig. 2** Two-week isolation rearing in F1 mice aggravates myelin and synapse impairments in the mPFC induced by paternal SI. **A–H** Representative immunohistology images (**A, C, E, G**) and the corresponding bar graphs with dots (**B, D, F, H**) showing MBP (**A, B**), NG2 (**C, D**), SYP (**E, F**), and PSD-95 (**G, H**) expression in the mPFC of mice (MBP, NG2, and SYP:  $n = 6$ ; PSD-95:  $n = 5$ ). Scale bar, 50  $\mu\text{m}$ . Representative Western blot (**I**) and the relevant quantified analysis (**J**) showing MBP, NG2, SYP, and PSD-95 protein levels in the mPFC of mice ( $n = 6$ ). Data are presented as mean  $\pm$  SEM and were analyzed by two-way ANOVA followed by Tukey's post hoc test.

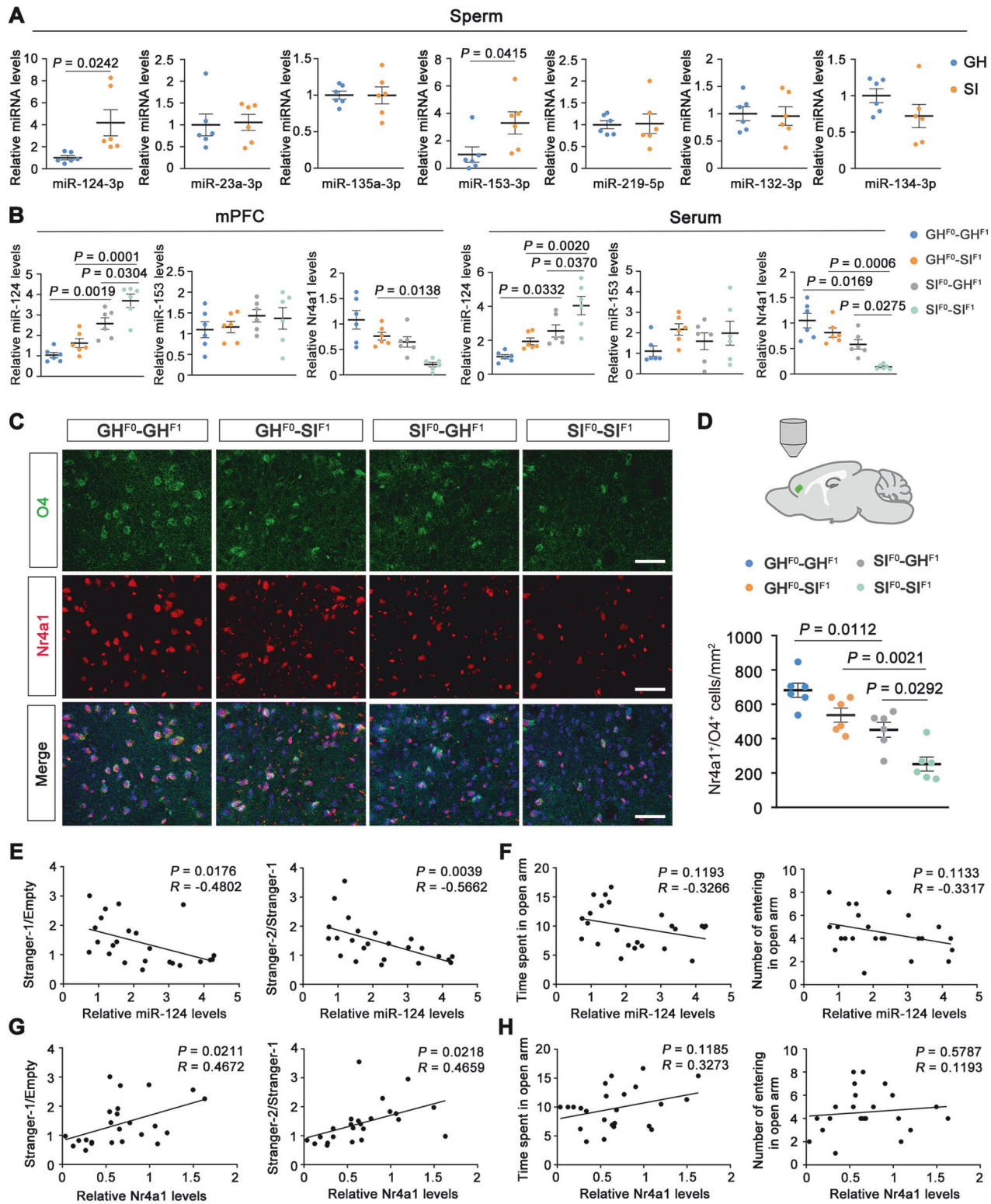


**Fig. 3 miR-124 regulates social behavior by targeting Nr4a1 in offspring of paternal SI. A** qRT-PCR evaluating miR-124-3p, miR-23a-3p, miR-135a-3p, miR-153-3p, miR-219-5p, miR-132-3p, and miR-134-3p levels in the sperm of GH and SI mice ( $n=6$ ). **B** qRT-PCR evaluating the expression of miR-153-3p, miR-124-3p, and its target gene *Nr4a1* in serum and the mPFC of F1 mice ( $n=6$ ). Representative immunofluorescence images (**C**) and the corresponding bar graphs with dots (**D**) showing *Nr4a1*<sup>+</sup>*O4*<sup>+</sup> cells in the mPFC of mice ( $n=6$ ). Scale bar, 50  $\mu$ m. **E–H** The correlation analysis of social behavior with miR-124 (**E**), anxiety-like phenotypes with miR-124 (**F**), social behavior with *Nr4a1* (**G**), and anxiety-like phenotypes with *Nr4a1* (**H**). Data are presented as mean  $\pm$  SEM and was analyzed by two-tailed Student's *t* test in **A**, and in **B** and **D** were analyzed by two-way ANOVA followed by Tukey's post hoc test. Correlating assays were conducted using the Spearman rank correlation test in **E–H**.

## Two-week isolation rearing in F1 mice exacerbates mPFC hypomyelination induced by paternal SI

Previous studies have revealed that the mPFC is a critical brain region involved in social behavior both in rodent and human [19, 20]. SI mice exhibit myelin abnormalities and synaptic protein loss in the mPFC [32, 33]. Therefore, we selected this

region to observe the pathological consequence of paternal early SI experiences on F1 mice with or without SI stress. EM results revealed reduced myelin thickness and impaired OLS maturation, as indicated by a decrease in heterochromatin area (Fig. 1G–I). Synaptic integrity was also altered, reflected by reduced postsynaptic density thickness and presynaptic active

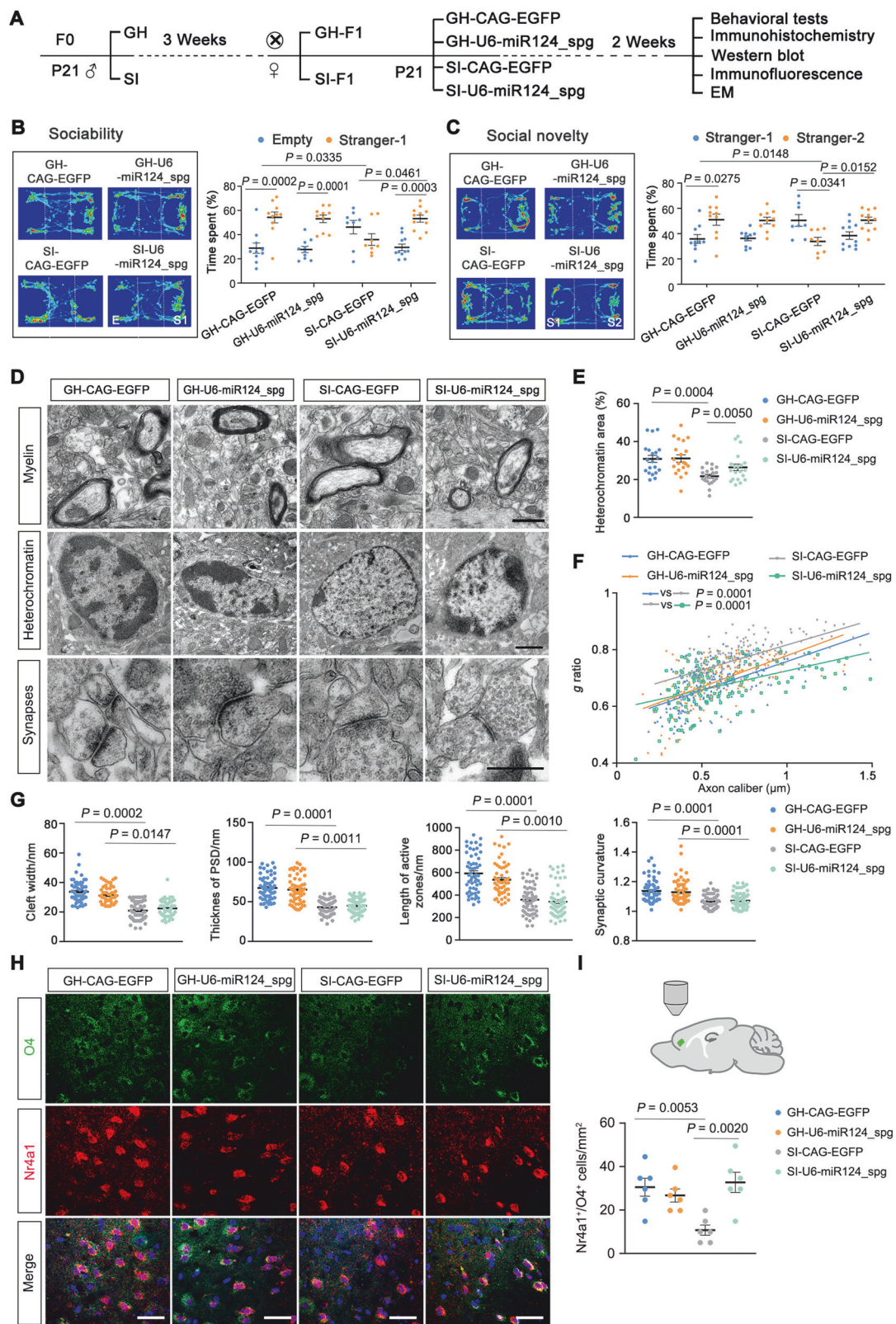


**Fig. 4 Inhibiting miR-124 in mPFC alleviates social behavior and myelinogenesis impairments caused by paternal SI.** **A** A timeline diagram showing weaned mice receiving AAV virus injection, group housing or isolation rearing, and behavioral tests. **B, C** Trajectory heat maps and statistical graph showing the percentage of time spent in each chamber during the three-chamber test (GH-CAG-EGFP:  $n = 10$ ; GH-U6-miR-124\_spg:  $n = 10$ ; SI-CAG-EGFP:  $n = 8$ ; SI-U6-miR-124\_spg:  $n = 11$ ). **D** Representative EM images showing myelin (top), OLs nuclear heterochromatin (middle), and synaptic morphology (bottom) in the mPFC of mice from the different groups. Scale bars, 500 nm. **E** Graph showing the area percentage of OLs nuclear heterochromatin in GH-CAG-EGFP (20 nuclei), GH-U6-miR-124\_spg (20 nuclei), SI-CAG-EGFP (20 nuclei), and SI-U6-miR-124\_spg (20 nuclei) mice ( $n = 5$ ). **F** Scatter plot of  $g$  ratios with linear least squares fitting in GH-CAG-EGFP (158 axons), GH-U6-miR-124\_spg (140 axons), SI-CAG-EGFP (169 axons), and SI-U6-miR-124\_spg (155 axons) mice ( $n = 5$ ). **G** Graphs showing quantification of PSD, synaptic cleft width, length of the active zones, and synaptic curvature in GH-CAG-EGFP (57 synapses), GH-U6-miR-124\_spg (59 synapses), SI-CAG-EGFP (60 synapses), and SI-U6-miR-124\_spg (65 synapses) mice ( $n = 5$ ). Representative immunofluorescence images (**H**) and the corresponding bar graphs with dots (**I**) showing  $\text{Nr}4\text{a}1^+$   $\text{O}4^+$  cells in the mPFC of mice ( $n = 6$ ). Data are presented as mean  $\pm$  SEM and were analyzed by three-way ANOVA followed by Tukey's multiple comparisons test in **B, C**, and others were analyzed by two-way ANOVA followed by Tukey's post hoc test.

zone length (Fig. 1G, J). Two-week isolation rearing in F1 mice aggravated mPFC hypomyelination induced by paternal SI (Fig. 1G–J). Consistently, both immunohistochemical staining and Western blot showed that, compared with  $\text{SI}^{\text{FO}}\text{-GH}^{\text{F}1}$  mice, MBP expression levels, rather than PSD-95 and SYP, were further reduced in the mPFC of  $\text{SI}^{\text{FO}}\text{-SI}^{\text{F}1}$  mice (Fig. 2A, B, E–J; Supplementary Fig. 2A, B).

Previous studies have also demonstrated that SI inhibits mPFC OPCs differentiating into mature OLs. The current results confirmed that paternal early experiences of isolation had a similar inhibitory effect on differentiation of OPCs, as evidenced by a high proportion of NG2-positive OPCs in the mPFC of F1 mice [34]; and 2-week isolation led to an increase in NG2-positive OPCs (Fig. 2C, D, I, J). Conversely, the 1-week isolation exposure did not exacerbate the aforementioned damages (Supplementary Fig. 3A–H). We also performed immunohistochemistry and Western blot to investigate the effect of paternal SI and/or isolation stress for 1 or 2 weeks on the expression levels of MBP, NG2, SYP, and PSD-95 in the hippocampus and amygdala, both of which are related to stress or anxiety-like behavior [5, 35, 36], and no significant changes were observed (Supplementary Fig. 4A–J; Supplementary Fig. 5A–J; Supplementary Fig. 6A–H and Supplementary Fig. 7A–H). Together, these results indicated that paternal early SI caused hypomyelination in the mPFC of F1 mice, and this pathological change was more pronounced after a relatively short isolation feeding period.

#### miR-124 regulates the behavior and pathology by targeting $\text{Nr}4\text{a}1$ in mPFC OLs of mice with paternal SI

The impact of parental adverse life experiences on their behavior and pathology can be transmitted to offspring through epigenetic mechanisms [37]. For example, paternal miR-449 or miR-34 in sperm can affect the behavioral phenotypes and neurodevelopment of the offspring through inheritance [38]. Our previous studies revealed a significant upregulation of miR-153-3p, miR-124-3p, miR-23a-3p, miR-135a-3p, and miR-219-5p expression levels in the mPFC of early SI mice [5]. In this study, qRT-PCR revealed a significant increase in miR-124-3p and miR-153-3p expression levels in the sperm of paternal SI mice (Fig. 3A; Supplementary Fig. 8A). The expression level of miR-124-3p, but not miR-153-3p, was significantly increased in the mPFC and the serum of F1 mice with paternal SI, and further upregulated in those with 2-week SI stress (Fig. 3B).

Our recent work has revealed the involvement of miR-124 in hypomyelination in the mPFC of early SI mice by targeting  $\text{Nr}4\text{a}1$  [5]. In this study, we confirmed that the parental SI caused a significant decrease in  $\text{Nr}4\text{a}1$  transcription levels both in the mPFC and the serum of F1 mice; and this downregulation was further pronounced after 2-week SI rearing (Fig. 3B). We have also confirmed that reduced  $\text{Nr}4\text{a}1$  expression in the OLs and OLs progenitors positive for O4 (Fig. 3C, D) [34]. Correlation analysis showed that the level of miR-124 or  $\text{Nr}4\text{a}1$  has negative and positive correlation with social behavior, but not with anxiety-like

behavior (Fig. 3E–H). These findings further indicated that miR-124 regulates social behaviors by targeting  $\text{Nr}4\text{a}1$  in mPFC OLs in F1 mice with paternal SI stimulation.

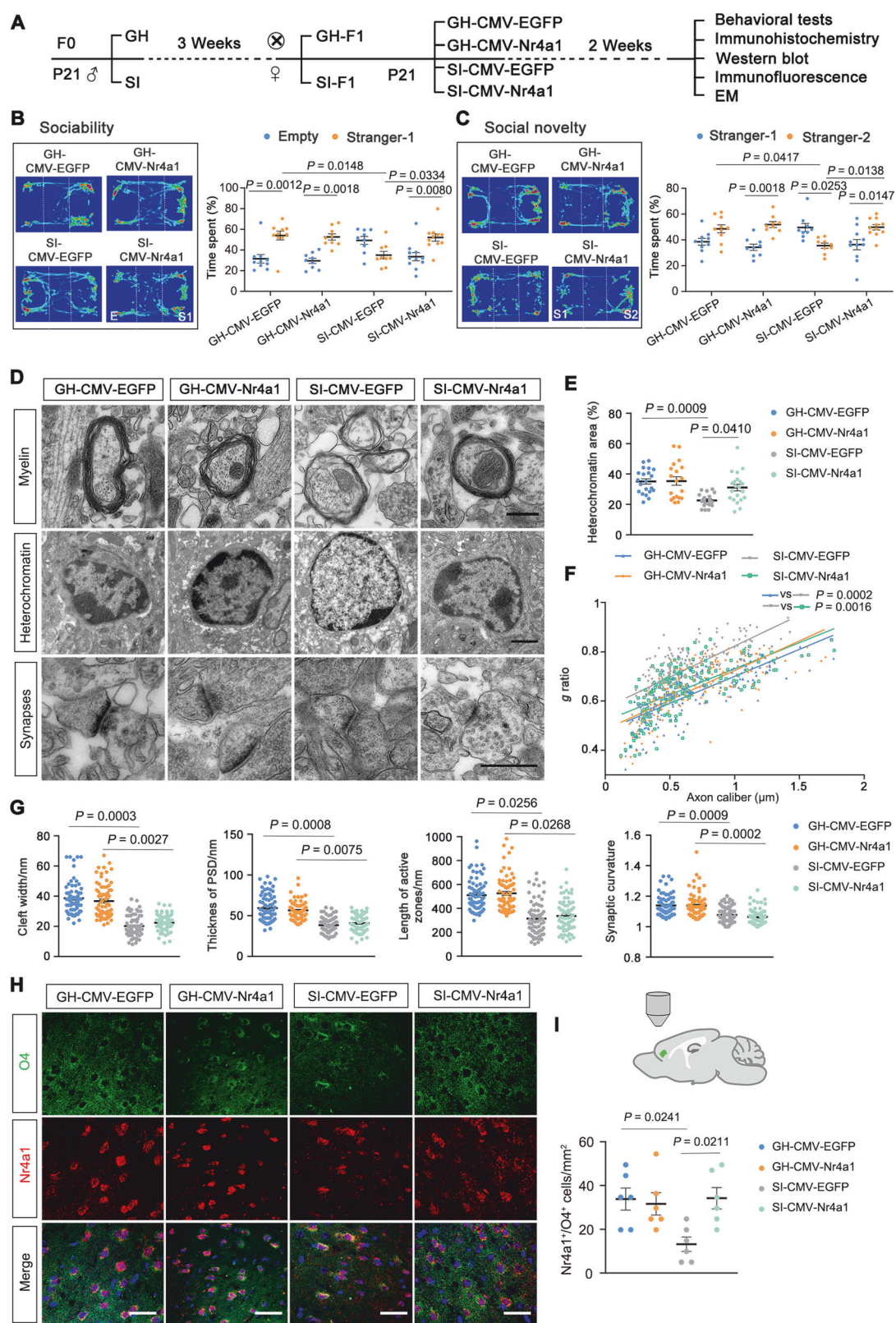
#### Inhibiting the effect of miR-124 on offspring mPFC ameliorates the impairments of social behavior and myelinogenesis induced by paternal SI rearing

To investigate the potential mechanism of miR-124/ $\text{Nr}4\text{a}1$  regulating of social behavior and mPFC myelination in F1 mice with paternal SI rearing, we used an AAV vector to target miR-124 expression in a miRNA sponge under the U6 promoter. The virus was injected into bilateral mPFC of F1 mice with paternal SI to inhibit the expression of miR-124 (Fig. 4A). Immunofluorescence demonstrated the accuracy of the injection site (Supplementary Fig. 8B) and Western blot validated the effectiveness of the virus by the increased expression of  $\text{Nr}4\text{a}1$  in the mPFC of SI-CAG-miR-124\_spg mice (Supplementary Fig. 8C). The behavioral tests revealed that inhibiting miR-124 expression improved social behavioral performance of F1 mice with paternal SI rearing (Fig. 4B, C), while short-term memory and anxiety-like phenotypes did not show significant changes (Supplementary Fig. 9A–F).

Consistently, EM results revealed that the expression of miR-124 sponge in the mPFC normalized OLs maturation and myelination in F1 mice with paternal SI (Fig. 4D–F). However, it did not improve mPFC synaptogenesis, as revealed by the lack of differences in synaptic parameters between SI-CAG-EGFP mice and SI-CAG-miR-124\_spg mice (Fig. 4D, G). These results were confirmed again by immunostaining and Western blot analysis of MBP, PSD-95, and SYP expression levels (Supplementary Fig. 10A–J). Immunofluorescence results showed that the inhibition of miR-124 expression led to an increase in the expression level of  $\text{Nr}4\text{a}1$  in mPFC OLs of SI-CAG-miR-124\_spg mice (Fig. 4H, I). In summary, miR-124 sponge expression in the mPFC can specifically alleviate social interaction deficits and hypomyelination in F1 mice with paternal SI rearing.

#### Overexpressing $\text{Nr}4\text{a}1$ in the mPFC improves social behavior and myelination of the mice with paternal SI rearing

In order to confirm the downregulation of  $\text{Nr}4\text{a}1$  expression in the mPFC contributing to social interaction defect in F1 mice with paternal SI, AAV, overexpressing  $\text{Nr}4\text{a}1$  under the CMV promoter (AAV-CMV- $\text{Nr}4\text{a}1$ -EGFP), was injected into bilateral mPFC of F1 mice (Fig. 5A). We observed clear EGFP signal in the mPFC (Supplementary Fig. 11A) and significantly elevated  $\text{Nr}4\text{a}1$  level in the mPFC (Supplementary Fig. 11B), indicating effective virus infection and successful expression of  $\text{Nr}4\text{a}1$ . The results showed that overexpression of  $\text{Nr}4\text{a}1$  rescued social behavior impairments in SI-CMV- $\text{Nr}4\text{a}1$  mice. At the same time, paternal SI rearing induced thinning of myelin sheath and reduced MBP expression were also partially corrected (Fig. 5B–G; Supplementary Fig. 12A–J). Similar to the miR-124 sponge expression, anxiety-like behavior and short-term working memory had no significant changes (Supplementary Fig. 13A–F). Immunofluorescence results



revealed that Nr4a1 expression was restored in mPFC OLs of SI-CMV-Nr4a1 mice (Fig. 5H, I). Taken together, these results suggested that overexpressing Nr4a1 in the mPFC of F1 mice could improve the impaired social behavior and myelin dysfunction caused by paternal SI rearing.

**SI for two weeks exacerbates the downregulation of GR expression in mPFC OLs in the mice with paternal isolation**  
 SI, as a unique social environmental stress, can activate the HPA axis, leading to an increase in serum Cort levels [39]. It is reported that the HPA axis is involved in the pathogenesis of anxiety like

**Fig. 5 Overexpressing Nr4a1 in mPFC alleviates social behavior and myelinogenesis impairments caused by paternal SI. A** A timeline diagram showing mice receiving weanling, AAV virus injection, group housing or isolation rearing, social interaction test, and other behavioral tests. **B, C** Trajectory heat maps and statistical graph showing the percentage of time spent in each chamber during the three-chamber test (GH-CMV-EGFP:  $n = 10$ ; GH-CMV-Nr4a1:  $n = 9$ ; SI-CMV-EGFP:  $n = 9$ ; SI-CMV-Nr4a1:  $n = 11$ ). **D** Representative EM images showing myelin (top), OLs nuclear heterochromatin (middle), and synaptic morphology (bottom) in the mPFC of mice from the different groups. Scale bars, 500 nm. **E** Graph showing the area percentage of OLs nuclear heterochromatin in GH-CMV-EGFP (21 nuclei), GH-CMV-Nr4a1 (19 nuclei), SI-CMV-EGFP (19 nuclei), and SI-CMV-Nr4a1 (21 nuclei) mice ( $n = 5$ ). **F** Scatter plot of  $g$  ratios with linear least squares fitting in GH-CMV-EGFP (169 axons), GH-CMV-Nr4a1 (171 axons), SI-CMV-EGFP (175 axons), and SI-CMV-Nr4a1 (178 axons) mice ( $n = 5$ ). **G** Graphs showing quantification of PSD, synaptic cleft width, length of the active zones, and synaptic curvature in GH-CMV-EGFP (72 synapses), GH-CMV-Nr4a1 (72 synapses), SI-CMV-EGFP (69 synapses), and SI-CMV-Nr4a1 (70 synapses) mice ( $n = 5$ ). Representative immunofluorescence images (**H**) and the corresponding bar graphs with dots (**I**) showing Nr4a1<sup>+</sup> O4<sup>+</sup> cells in the mPFC of mice ( $n = 6$ ). Data are presented as mean  $\pm$  SEM and were analyzed by three-way ANOVA followed by Tukey's multiple comparisons test in **B, C**, and others were analyzed by two-way ANOVA followed by Tukey's post hoc test.

behavior [40]. Anxiety patients exhibit higher level of cortisol [41]. Moreover, the offspring mice whose parent were exposed to chronic social defeat stress exhibited increased depressive- and anxiety-like behaviors, accompanied by a significant increase in serum cortisol level [12]. This study found that the number of GR<sup>+</sup> cells in the mPFC decreased in F1 mice with paternal SI rearing, and 2-week SI further exacerbated the loss of GR<sup>+</sup> NG2<sup>+</sup> OLs without affecting GR<sup>+</sup> NeuN<sup>+</sup> neurons (Fig. 6A–F).

Alterations in GR level led to dysregulation of the HPA axis, causing an increase in serum Cort level [42]. In this study, we found that offspring with paternal isolation rearing showed high level of Cort in the serum detected by ELISA. Meanwhile, compared to the SI<sup>F0</sup>-GH<sup>F1</sup> group, the SI<sup>F0</sup>-SI<sup>F1</sup> group had a higher Cort level (Fig. 6G). Moreover, inhibiting the effect of miR-124 in the mPFC of SI<sup>F0</sup>-GH<sup>F1</sup> mice reduced serum Cort and improved GR expression in mPFC OLs rather than neurons (Supplementary Fig. 14A–F). The overexpression of Nr4a1 in the mPFC of SI<sup>F0</sup>-GH<sup>F1</sup> mice had similar effects on serum Cort and GR expression (Supplementary Fig. 15A–F). Therefore, the decrease in GR level in mPFC OLs might be involved in regulating the social behavior and pathological effects of F1 mice with paternal SI rearing.

Finally, we conducted *in vitro* experiments to confirm the damage effect of high Cort exposure on cultured OLs and neurons. As expected, the cultured OLs with Cort (10 nM) treatment showed decreases in branch length and total number of intersections, as shown by immunofluorescence staining (Fig. 6H–J). Treating primary cortical neurons with Cort for 48 hours also resulted in a significant decrease in the total length of neurites (Fig. 6K, L). In addition, qRT-PCR experiments revealed that Cort exposure reduced the levels of MBP in OLs and SYP in neurons, respectively (Fig. 6M, N).

In summary, our findings suggested that paternal SI increased the level of miR-124 in the mPFC of F1 mice through epigenetic modifications, negative regulating the expression levels of Nr4a1 and GR in OLs. This change might further influence the serum levels of Cort, exacerbating synaptic and myelin damage in the mPFC of F1 mice. These alterations, in turn, affected the social abilities of offspring (Fig. 7).

## DISCUSSION

Adverse life experiences during childhood, such as social neglect and isolation, increase the risk of developing anxiety, depression, and PTSD during adulthood [43, 44]. The impact of parental adverse life experiences and psychological disorders on offspring has also been widely concerned [30, 32]. In the current study, the F1 mice with paternal SI rearing demonstrated that social interaction impairments and increased anxiety-like phenotype, accompanied by abnormalities in myelin and synapses in the mPFC. Moreover, social interaction impairments and hypomyelination in the mPFC were further exacerbated in 2-week SI. These findings suggested that paternal SI rearing is sufficient to cause

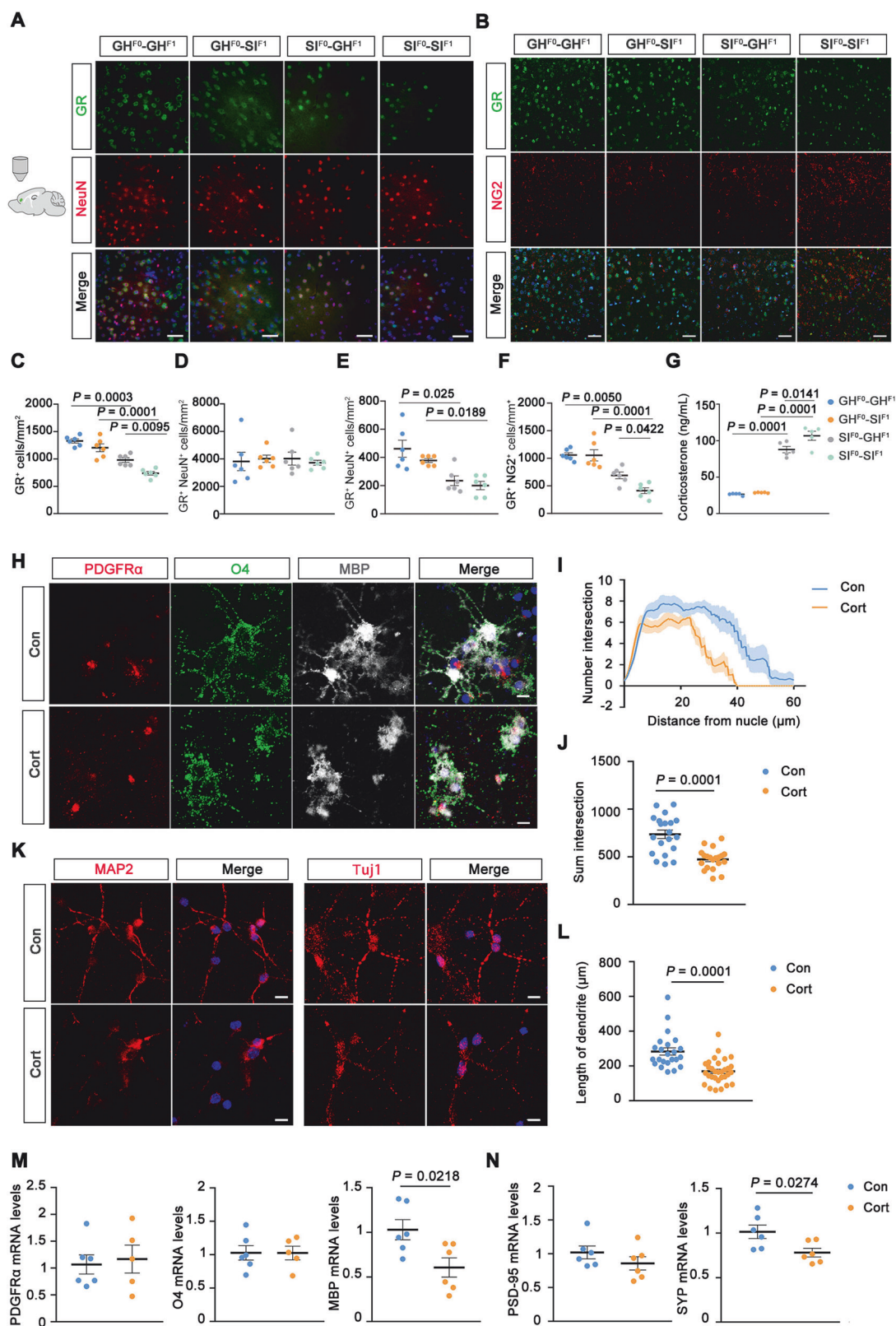
social withdrawal behavior and hinder myelination during the development of F1 offspring, making them more susceptible to isolation stress.

Numerous lines of evidence suggest that offspring of parents with mental health issues or serious mental illnesses are at increased risk of anxiety-like phenotypes, obsessive-compulsive disorders, autism spectrum disorders, attention deficits, and hyperactivity disorders [7, 45]. The present results showed that F1 mice with fathers suffering from SI reduced preference for social novelty, and 2 weeks of SI exposure further exacerbated social novelty deficits and myelination impairments, while having limited effects on anxiety-like phenotypes and synaptic development. This may be attributed to the completion of synaptogenesis in the development brain in mice at the age of 3 weeks, whereas myelin formation persists until adolescence [46]. In addition, myelination in the mPFC is influenced by social experiences [47] and its alterations in turn affect the social behavior of adolescent mice [32, 48]. Therefore, F1 mice with parental SI specifically showed that their social ability was more susceptible to isolation impairment.

Multiple brain regions are involved in regulating social interaction behavior and anxiety-like phenotypes, including the mPFC, orbitofrontal cortex, anterior cingulate cortex, hippocampus, amygdala, temporo-parietal junction, and superior temporal gyrus [49, 50]. This study revealed that F1 mice with paternal SI rearing caused significant damage to myelin and synaptic proteins in the mPFC, but did not show significant difference in the hippocampus and amygdala. These findings indicated that the influence of paternal SI on different brain regions is heterogeneous, and further research is needed to elucidate the related neural circuits involving in this process.

miRNAs are a class of non-coding regulatory small RNAs that play a crucial role in brain development and neuropsychiatric disorders [51, 52]. miR-124 is a widely expressed miRNA in the brain, playing a crucial role in neuronal development and brain function. For examples, miR-124 regulates cocaine induced plasticity in rats by targeting brain-derived neurotrophic factor (BDNF), which plays a central role in reward and memory [53].

It is worth noting that miR-124 is involved in depression [54, 55]. Patients with depression often exhibit severe social withdrawal behavior. Postmortem analysis of individuals with severe depression show an elevated level of has-miR-124 in the BA46 brain region [55]. miR-124 has been reported to modulate depression-like phenotypes in mice by targeting GR in the testis and influencing the BDNF/TrkB/CREB signaling pathway [54]. Furthermore, miR-124 participates in prenatal dexamethasone exposure by targeting HDAC5, reducing testosterone synthesis in offspring rats and affecting the fertility of male mice [56]. Our recent work has also revealed a pivotal role of the miR-124/Nr4a1 pathway in regulating myelination in the mPFC of mice with early SI experiences [5]. The present results further demonstrated dysregulated miR-124 contributes to impaired social memory behavior caused by paternal early SI. Together, these data further



supported miR-124 is necessary for maintaining brain function of mice and their offspring.

The current study also revealed that SI significantly increases the expression of miR-124 in the sperm of mice. Indeed, increasing evidence suggests that the social stress experienced by fathers

can be transmitted to their offspring through RNA molecules in the sperm [57, 58]. Early adverse life experiences exhibited alterations in dozens of small RNA molecules in the sperm of mice [37]. The current results provided the new evidence that transgenerational epigenetic programming via sperm miRNA is

**Fig. 6 Two-week isolation rearing in F1 mice increases serum Cort levels and down-regulates GR expression in OLs caused by paternal SI.** Representative immunofluorescence images showing GR expression in NeuN<sup>+</sup> neurons (**A**) and NG2<sup>+</sup> OLs (**B**) in the mPFC of mice. Scale bar, 50  $\mu$ m. The GR (**C**), NeuN<sup>+</sup> (**D**), GR<sup>+</sup> NeuN<sup>+</sup> (**E**) and GR<sup>+</sup> NG2<sup>+</sup> (**F**) expression cells in the mPFC of mice ( $n = 6$ ). **G** Serum Cort detected by ELISA ( $n = 5$ ). **H** Primary OLs were incubated with 10 nM Cort for 48 hours. The expression of MBP and O4 was detected by immunofluorescence. Scale bar, 20  $\mu$ m. **I, J** Sholl analysis identified that Cort reduced branch length and sum intersection of OLs in cultured OLs (20 cells for control and 20 cells for Cort) ( $n = 6$ , at least 2 different cells are randomly selected from each well). **K** Primary cortical neurons were incubated with 10 nM Cort for 48 h. The expression of MAP2 and Tuj1 was detected by immunofluorescence. Scale bar, 20  $\mu$ m. **L** NeuroAnatomy analysis identified that Cort reduced the length of dendrites of neurons in cultured neurons (24 cells for control and 31 cells for Cort) ( $n = 6$ , at least 2 different cells are randomly selected from each well). **M** qRT-PCR evaluating altered expression of differentiating markers of OLs by incubated with 10 nM Cort for 48 h in primary OLs ( $n = 6$ ). **N** qRT-PCR evaluating altered expression of neuron markers by incubated with 10 nM Cort for 48 h in primary cortical neurons ( $n = 6$ ). Data are presented as mean  $\pm$  SEM. Data in **C-G** were analyzed by two-way ANOVA followed by Tukey's post hoc test and in **J-N** were analyzed by two tailed Student's *t* test.

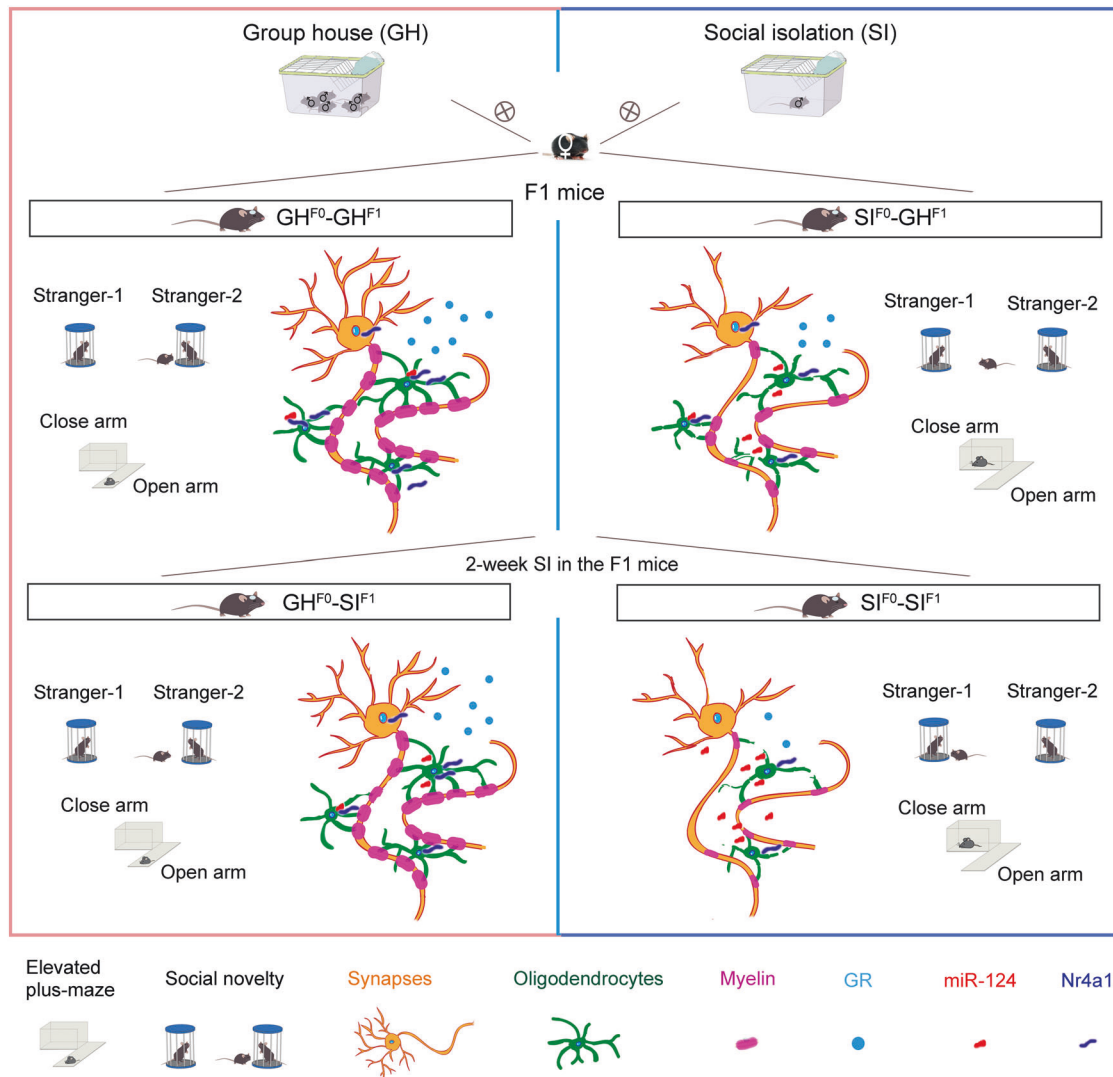


**Fig. 7** Two-week isolation rearing in F1 mice exacerbates myelin impairments caused by paternal SI, through modulating miR-124, negatively regulating Nr4a1 and GR in OLs, and therefore affects social novelty behavior.

sufficient to transmit intergenerational stress and program neurodevelopment. However, the roles of other common epigenetics, such as methylation and histone modification in neuropsychiatric alterations of SI mice and their offspring remain to be determined.

Dysregulation of the HPA axis is closely related to behavioral deficits and emotional disorders [59]. Cort inhibits the proliferation of OPCs in both white and gray matter regions of adult rat brain [60]. This study found that after 2-week isolation rearing in F1 mice

with paternal SI, serum Cort levels increased and GR expression in OLs decreased, while GR level in neurons did not have a significant impact. SI, as a stressor causing elevated serum Cort expression, inhibits the differentiation of OLs and myelin sheaths in the mPFC. This may be the significant pathological basis for social novelty disorders and anxiety-like phenotypes in F1 mice. However, other factors, such as differences in gut microbial composition between SI model mice and unstimulated controls, cannot be excluded as potential contributors to behavioral alterations in the offspring.

[61, 62]. Previous studies have found that maternal separation induces depressive-like phenotype and alters the behavioral response of isolated animals to aversive environments during the adulthood [31]. This further indicate that different forms of negative stress can lead to different behavioral abnormalities in offspring at different stages of life, and its potential complex mechanisms are worth further research.

The molecular basis of sperm miRNAs mediated intergenerational inheritance is gradually being addressed, although the mechanism is not fully understood. Recent research has found that factors such as psychological trauma and environmental stress can lead to changes in sperm miR-375, resulting in reduced fear and avoidance behavior and glucose metabolism disorders in offspring [63]. This effect is accompanied by epigenetic changes involving histone post-translational modifications at the mineralocorticoid receptor (MR) gene and decreased MR expression in the hippocampus [64]. miRNAs in sperm may regulate genes related to the development of the nervous system in the early embryos, leading to offspring developing symptoms of depression in adulthood [37]. Under stressful conditions, miR-124 is typically upregulated as a stabilizer of the transcriptome homeostatic state. In cultured neurons, transfection, KCl, and kainite acid stimulation significantly increase the expression of miR-124 [65]. It is worth noting that maternal separation enhances depression-like behaviors in young adult rats repeated restraint stress exposure, which is associated with up regulated expression of several repressor element-1 silencing transcription factor-4 target genes in the mPFC, including miR-124 [66]. Consistently, the current results revealed increased miR-124 in paternal sperm of SI mice as well as the mPFC of their F1 offspring, however, the exact epigenetic mechanism warrants further investigation.

In addition, in this study we did not observe the effects of early SI on F2 and F3 phenotypes. Epidemiological studies have found that the grandchildren (F2) of holocaust survivors have a higher risk of developing mental illnesses [67]. Protein restricted diets in the parental generation lead to reduced birth and brain weight in the offspring generation and alter glucose metabolism in unstimulated F2 individuals [68]. Furthermore, parental exposure to environmental factors may persist into the F2 generation and increase the susceptibility of multiple generations to adult-onset diseases such as diabetes [69]. Similarly, a study in rats found that maternal SI can lead to decreased exploratory behavior and changes in plasma phosphocreatine and glucose energy metabolism levels in F3 rats [70]. Additionally, SI of pregnant rats can induce changes in intrauterine inflammation, which can be transmitted to the F3 generation, and an enriched environment does not improve uterine inflammation changes in F1-F3 generations [71]. These studies suggested that stress stimuli may have a certain impact on multiple generations. However, the F2-F3 generation effects of adverse social stress in this study need to be further clarified.

In conclusion, our findings documented the detrimental effects of paternal early SI rearing on social behavioral establishment in F1 mice and revealed a novel role of miR-124/Nr4a1 signaling in transmitting intergenerational stress and programing neurodevelopment. This discovery contributes to a broader understanding of the negative impact of early negative experiences on future generations. Especially in the stage soon after the COVID-19 pandemic, individuals will inevitably experience different SI durations. The impact of this isolation on individuals themselves and their descendants warrants further investigation in the future.

## DATA AVAILABILITY

All data generated or analyzed during this study are included in this published article and its supplementary information files.

## REFERENCES

- Holt-Lunstad J. Why Social Relationships Are Important for Physical Health: A Systems Approach to Understanding and Modifying Risk and Protection. *Annu Rev Psychol.* 2018;69:437–58. <https://doi.org/10.1146/annurev-psych-122216-011902>.
- Kempermann G. Environmental enrichment, new neurons and the neurobiology of individuality. *Nat Rev Neurosci.* 2019;20:235–45. <https://doi.org/10.1038/s41583-019-0120-x>.
- Burke AR, McCormick CM, Pellis SM, Lukkes JL. Impact of adolescent social experiences on behavior and neural circuits implicated in mental illnesses. *Neurosci Biobehav Rev.* 2017;76:280–300. <https://doi.org/10.1016/j.neubiorev.2017.01.018>.
- Tzanoulinou S, Sandi C. The Programming of the Social Brain by Stress During Childhood and Adolescence: From Rodents to Humans. *Curr Top Behav Neurosci.* 2017;30:411–29. [https://doi.org/10.1007/7854\\_2015\\_430](https://doi.org/10.1007/7854_2015_430).
- Zhang Y, Pang Y, Feng W, Jin Y, Chen S, Ding S, et al. miR-124 regulates early isolation-induced social abnormalities via inhibiting myelinogenesis in the medial prefrontal cortex. *Cell Mol Life Sci.* 2022;79:507. <https://doi.org/10.1007/s00018-022-04533-6>.
- Mychasiuk R, Metz GA. Epigenetic and gene expression changes in the adolescent brain: What have we learned from animal models? *Neurosci Biobehav Rev.* 2016;70:189–97. <https://doi.org/10.1016/j.neubiorev.2016.07.013>.
- Davidson KA, Munk-Laursen T, Foli-Andersen P, Ranning A, Harder S, Nordentoft M, et al. Mental and pediatric disorders among children 0–6 years of parents with severe mental illness. *Acta Psychiatr Scand.* 2022;145:244–54. <https://doi.org/10.1111/acps.13358>.
- Shepherd-Banigan M, Kelley ML, Katon JG, Curry JF, Goldstein KM, Brancu M, et al. Paternal history of mental illness associated with posttraumatic stress disorder among veterans. *Psychiatry Res.* 2017;256:461–8. <https://doi.org/10.1016/j.jpsychires.2017.06.053>.
- Lewis G, Neary M, Polek E, Flouri E, Lewis G. The association between paternal and adolescent depressive symptoms: evidence from two population-based cohorts. *Lancet Psychiatry.* 2017;4:920–6. [https://doi.org/10.1016/S2215-0366\(17\)30408-X](https://doi.org/10.1016/S2215-0366(17)30408-X).
- Stein A, Pearson RM, Goodman SH, Rapa E, Rahman A, McCallum M, et al. Effects of perinatal mental disorders on the fetus and child. *Lancet.* 2014;384:1800–19. [https://doi.org/10.1016/S0140-6736\(14\)61277-0](https://doi.org/10.1016/S0140-6736(14)61277-0).
- Yehuda R, Bierer LM. Transgenerational transmission of cortisol and PTSD risk. *Prog Brain Res.* 2008;167:121–35. [https://doi.org/10.1016/S0079-6123\(07\)67009-5](https://doi.org/10.1016/S0079-6123(07)67009-5).
- Dietz DM, Laplant Q, Watt EL, Hodes GE, Russo SJ, Feng J, et al. Paternal transmission of stress-induced pathologies. *Biol Psychiatry.* 2011;70:408–14. <https://doi.org/10.1016/j.biopsych.2011.05.005>.
- Braun K, Champagne FA. Paternal influences on offspring development: behavioural and epigenetic pathways. *J Neuroendocrinol.* 2014;26:697–706. <https://doi.org/10.1111/jne.12174>.
- Rodgers AB, Morgan CP, Leu NA, Bale TL. Transgenerational epigenetic programming via sperm microRNA recapitulates effects of paternal stress. *Proc Natl Acad Sci USA.* 2015;112:13699–704. <https://doi.org/10.1073/pnas.1508347112>.
- Chan JC, Morgan CP, Adrian Leu N, Shetty A, Cisse YM, Nugent BM, et al. Reproductive tract extracellular vesicles are sufficient to transmit intergenerational stress and program neurodevelopment. *Nat Commun.* 2020;11:1499. <https://doi.org/10.1038/s41467-020-15305-w>.
- Short AK, Fennell KA, Perreau VM, Fox A, O'Bryan MK, Kim JH, et al. Elevated paternal glucocorticoid exposure alters the small noncoding RNA profile in sperm and modifies anxiety and depressive phenotypes in the offspring. *Transl Psychiatry.* 2016;6:e837. <https://doi.org/10.1038/tp.2016.109>.
- He N, Kong QQ, Wang JZ, Ning SF, Miao YL, Yuan HJ, et al. Parental life events cause behavioral difference among offspring: Adult pre-gestational restraint stress reduces anxiety across generations. *Sci Rep.* 2016;6:39497. <https://doi.org/10.1038/srep39497>.
- Rodgers AB, Morgan CP, Bronson SL, Revello S, Bale TL. Paternal stress exposure alters sperm microRNA content and reprograms offspring HPA stress axis regulation. *J Neurosci.* 2013;33:9003–12. <https://doi.org/10.1523/JNEUROSCI.0914-13.2013>.
- Ligneul R, Obeso I, Ruff CC, Dreher JC. Dynamical Representation of Dominance Relationships in the Human Rostromedial Prefrontal Cortex. *Curr Biol.* 2016;26:3107–15. <https://doi.org/10.1016/j.cub.2016.09.015>.
- Zhou T, Zhu H, Fan Z, Wang F, Chen Y, Liang H, et al. History of winning remodels thalamo-PFC circuit to reinforce social dominance. *Science.* 2017;357:162–8. <https://doi.org/10.1126/science.aak9726>.
- Shimizu S, Tanaka T, Tohyama M, Miyata S. Yokokansan normalizes glucocorticoid receptor protein expression in oligodendrocytes of the corpus callosum by regulating microRNA-124a expression after stress exposure. *Brain Res Bull.* 2015;114:49–55. <https://doi.org/10.1016/j.brainresbull.2015.03.007>.
- Kaidanovich-Beilin O, Lipina T, Vukobradovic I, Roder J, Woodgett JR. Assessment of social interaction behaviors. *J Vis Exp.* 2011;25:2473. <https://doi.org/10.3791/2473>.
- Rezaie M, Nasehi M, Vaseghi S, Mohammadi-Mahdabadi-Hasani MH, Zarrindast MR, Nasiri Khalili MA. The protective effect of alpha lipoic acid (ALA) on social

- interaction memory, but not passive avoidance in sleep-deprived rats. *Naunyn Schmiedebergs Arch Pharmacol.* 2020;393:2081–91. <https://doi.org/10.1007/s00210-020-01916-z>.
24. Kraeuter AK, Guest PC, Sarnyai Z. The Open Field Test for Measuring Locomotor Activity and Anxiety-Like Behavior. *Methods Mol Biol.* 2019;1916:99–103. [https://doi.org/10.1007/978-1-4939-8994-2\\_9](https://doi.org/10.1007/978-1-4939-8994-2_9).
  25. Ari C, D'Agostino DP, Diamond DM, Kindy M, Park C, Kovacs Z. Elevated Plus Maze Test Combined with Video Tracking Software to Investigate the Anxiolytic Effect of Exogenous Ketogenic Supplements. *J Vis Exp.* 2019; 7. <https://doi.org/10.3791/58396>.
  26. Cleal M, Fontana BD, Ranson DC, McBride SD, Swinny JD, Redhead ES, et al. The Free-movement pattern Y-maze: A cross-species measure of working memory and executive function. *Behav Res Methods.* 2021;53:536–57. <https://doi.org/10.3758/s13428-020-01452-x>.
  27. Zhang Y, Feng W, Wang Z, Pang Y, Jin Y, Chen S, et al. Early growth response 2 in the mPFC regulates mouse social and cooperative behaviors. *Lab Anim (NY).* 2023;52:37–50. <https://doi.org/10.1038/s41684-022-01090-0>.
  28. Wang Z, Zhang Y, Feng W, Pang Y, Chen S, Ding S, et al. Miconazole Promotes Cooperative Ability of a Mouse Model of Alzheimer Disease. *Int J Neuropsychopharmacol.* 2022;25:951–67. <https://doi.org/10.1093/ijnp/pyac061>.
  29. Liu J, Dietz K, DeLoyht JM, Pedre X, Kelkar D, Kaur J, et al. Impaired adult myelination in the prefrontal cortex of socially isolated mice. *Nat Neurosci.* 2012;15:1621–3. <https://doi.org/10.1038/nn.3263>.
  30. Bohacek J, Mansuy IM. A guide to designing germline-dependent epigenetic inheritance experiments in mammals. *Nat Methods.* 2017;14:243–9. <https://doi.org/10.1038/nmeth.4181>.
  31. Franklin TB, Russig H, Weiss IC, Graff J, Linder N, Michalon A, et al. Epigenetic transmission of the impact of early stress across generations. *Biol Psychiatry.* 2010;68:408–15. <https://doi.org/10.1016/j.biopsych.2010.05.036>.
  32. Makinodan M, Rosen KM, Ito S, Corfas G. A critical period for social experience-dependent oligodendrocyte maturation and myelination. *Science.* 2012;337:1357–60. <https://doi.org/10.1126/science.1220845>.
  33. Zhang MQ, Ji MH, Zhao QS, Jia M, Qiu LL, Yang JJ, et al. Neurobehavioural abnormalities induced by repeated exposure of neonatal rats to sevoflurane can be aggravated by social isolation and enrichment deprivation initiated after exposure to the anaesthetic. *Br J Anaesth.* 2015;115:752–60. <https://doi.org/10.1093/bja/aev339>.
  34. Traiffort E, Zakaria M, Laouarem Y, Ferent J. Hedgehog: A Key Signaling in the Development of the Oligodendrocyte Lineage. *J Dev Biol.* 2016; 4. <https://doi.org/10.3390/jdb4030028>.
  35. Zhang X, Liu Y, Hong X, Li X, Meshul CK, Moore C, et al. NG2 glia-derived GABA release tunes inhibitory synapses and contributes to stress-induced anxiety. *Nat Commun.* 2021;12:5740. <https://doi.org/10.1038/s41467-021-25956-y>.
  36. Tye KM, Prakash R, Kim SY, Fenno LE, Grosenick L, Zarabi H, et al. Amygdala circuitry mediating reversible and bidirectional control of anxiety. *Nature.* 2011;471:358–62. <https://doi.org/10.1038/nature09820>.
  37. Wang Y, Chen ZP, Hu H, Lei J, Zhou Z, Yao B, et al. Sperm microRNAs confer depression susceptibility to offspring. *Sci Adv.* 2021;7. <https://doi.org/10.1126/sciadv.abd7605>.
  38. Dickson DA, Paulus JK, Mensah V, Lem J, Saavedra-Rodriguez L, Gentry A, et al. Reduced levels of miRNAs 449 and 34 in sperm of mice and men exposed to early life stress. *Transl Psychiatry.* 2018;8:101. <https://doi.org/10.1038/s41398-018-0146-2>.
  39. Li H, Xia N. The role of oxidative stress in cardiovascular disease caused by social isolation and loneliness. *Redox Biol.* 2020;37:101585. <https://doi.org/10.1016/j.redox.2020.101585>.
  40. Tafet GE, Nemeroff CB. Pharmacological Treatment of Anxiety Disorders: The Role of the HPA Axis. *Front Psychiatry.* 2020;11:443. <https://doi.org/10.3389/fpsyg.2020.00443>.
  41. Joels M, Karst H, Sarabdjitsingh RA. The stressed brain of humans and rodents. *Acta Physiol.* 2018;223:e13066. <https://doi.org/10.1111/apha.13066>.
  42. Laryea G, Muglia L, Arnett M, Muglia LJ. Dissection of glucocorticoid receptor-mediated inhibition of the hypothalamic-pituitary-adrenal axis by gene targeting in mice. *Front Neuroendocrinol.* 2015;36:150–64. <https://doi.org/10.1016/j.yfrne.2014.09.002>.
  43. Zhou C, Sylvia S, Zhang L, Luo R, Yi H, Liu C, et al. China's Left-Behind Children: Impact Of Parental Migration On Health, Nutrition, And Educational Outcomes. *Health Aff.* 2015;34:1964–71. <https://doi.org/10.1377/hlthaff.2015.0150>.
  44. Fuhrmann D, Knoll LJ, Blakemore SJ. Adolescence as a Sensitive Period of Brain Development. *Trends Cogn Sci.* 2015;19:558–66. <https://doi.org/10.1016/j.tics.2015.07.008>.
  45. Ayano G, Betts K, Lin A, Tait R, Alati R. Associations of maternal and paternal mental health problems with offspring anxiety at age 20 years: Findings from a population-based prospective cohort study. *Psychiatry Res.* 2021;298:113781. <https://doi.org/10.1016/j.psychres.2021.113781>.
  46. Dubois J, Dehaene-Lambertz G, Kulikova S, Poupon C, Huppi PS, Hertz-Pannier L. The early development of brain white matter: a review of imaging studies in fetuses, newborns and infants. *Neuroscience.* 2014;276:48–71. <https://doi.org/10.1016/j.neuroscience.2013.12.044>.
  47. Xin W, Chan JR. Myelin plasticity: sculpting circuits in learning and memory. *Nat Rev Neurosci.* 2020;21:682–94. <https://doi.org/10.1038/s41583-020-00379-8>.
  48. Cao M, Hu PP, Zhang YL, Yan YX, Shields CB, Zhang YP, et al. Enriched physical environment reverses spatial cognitive impairment of socially isolated APPswe/PS1dE9 transgenic mice before amyloidosis onset. *CNS Neurosci Ther.* 2018;24:202–11. <https://doi.org/10.1111/cns.12790>.
  49. Li Y, Mathis A, Grewe BF, Osterhout JA, Ahanonu B, Schnitzer MJ, et al. Neuronal Representation of Social Information in the Medial Amygdala of Awake Behaving Mice. *Cell.* 2017;171:1176–90.e1117. <https://doi.org/10.1016/j.cell.2017.10.015>.
  50. Jennings JH, Kim CK, Marshel JH, Raffee M, Ye L, Quirin S, et al. Interacting neural ensembles in orbitofrontal cortex for social and feeding behaviour. *Nature.* 2019;565:645–9. <https://doi.org/10.1038/s41586-018-0866-8>.
  51. Zhao J, Zhou Y, Guo M, Yue D, Chen C, Liang G, et al. MicroRNA-7: expression and function in brain physiological and pathological processes. *Cell Biosci.* 2020;10:77. <https://doi.org/10.1186/s13578-020-00436-w>.
  52. Nguyen LS, Fregeac J, Bole-Feysot C, Cagnard N, Iyer A, Anink J, et al. Role of miR-146a in neural stem cell differentiation and neural lineage determination: relevance for neurodevelopmental disorders. *Mol Autism.* 2018;9:38. <https://doi.org/10.1186/s13229-018-0219-3>.
  53. Chandrasekar V, Dreyer JL. microRNAs miR-124, let-7d and miR-181a regulate cocaine-induced plasticity. *Mol Cell Neurosci.* 2009;42:350–62. <https://doi.org/10.1016/j.mcn.2009.08.009>.
  54. Wang SS, Mu RH, Li CF, Dong SQ, Geng D, Liu Q, et al. microRNA-124 targets glucocorticoid receptor and is involved in depression-like behaviors. *Prog Neuropsychopharmacol Biol Psychiatry.* 2017;79:417–25. <https://doi.org/10.1016/j.pnpbp.2017.07.024>.
  55. Roy B, Dunbar M, Shelton RC, Dwivedi Y. Identification of MicroRNA-124-3p as a Putative Epigenetic Signature of Major Depressive Disorder. *Neuropsychopharmacology.* 2017;42:864–75. <https://doi.org/10.1038/npp.2016.175>.
  56. Liu M, Liu Y, Pei LG, Zhang Q, Xiao H, Chen YW, et al. Prenatal dexamethasone exposure programs the decreased testosterone synthesis in offspring rats by low level of endogenous glucocorticoids. *Acta Pharmacol Sin.* 2022;43:1461–72. <https://doi.org/10.1038/s41401-021-00789-z>.
  57. Sharma U, Rando OJ. Father-son chats: inheriting stress through sperm RNA. *Cell Metab.* 2014;19:894–5. <https://doi.org/10.1016/j.cmet.2014.05.015>.
  58. Rando OJ. Daddy issues: paternal effects on phenotype. *Cell.* 2012;151:702–8. <https://doi.org/10.1016/j.cell.2012.10.020>.
  59. Gao ZY, Chen TY, Yu TT, Zhang LP, Zhao SJ, Gu XY, et al. Cinnamaldehyde prevents intergenerational effect of paternal depression in mice via regulating GR/miR-190b/BDNF pathway. *Acta Pharmacol Sin.* 2022;43:1955–69. <https://doi.org/10.1038/s41401-021-00831-0>.
  60. Alonso G. Prolonged corticosterone treatment of adult rats inhibits the proliferation of oligodendrocyte progenitors present throughout white and gray matter regions of the brain. *Glia.* 2000;31:219–31. [https://doi.org/10.1002/1098-136\(200009\)31<219::aid-glia30>3.0.co;2-r](https://doi.org/10.1002/1098-136(200009)31<219::aid-glia30>3.0.co;2-r).
  61. Lim AI, McFadden T, Link VM, Han SJ, Karlsson RM, Stacy A, et al. Prenatal maternal infection promotes tissue-specific immunity and inflammation in offspring. *Science.* 2021;373. <https://doi.org/10.1126/science.abf3002>.
  62. Gawlinska K, Gawlinski D, Filip M, Przegalinski E. Relationship of maternal high-fat diet during pregnancy and lactation to offspring health. *Nutr Rev.* 2021;79:709–25. <https://doi.org/10.1093/nutrit/nuaa020>.
  63. Gapp K, Jawaid A, Sarkies P, Bohacek J, Pelczar P, Prados J, et al. Implication of sperm RNAs in transgenerational inheritance of the effects of early trauma in mice. *Nat Neurosci.* 2014;17:667–9. <https://doi.org/10.1038/nn.3695>.
  64. Gapp K, Soldado-Magraner S, Alvarez-Sanchez M, Bohacek J, Vernaz G, Shu H, et al. Early life stress in fathers improves behavioural flexibility in their offspring. *Nat Commun.* 2014;5:5466. <https://doi.org/10.1038/ncomms6466>.
  65. Manakov SA, Morton A, Enright AJ, Grant SG. A Neuronal Transcriptome Response Involving Stress Pathways is Buffered by Neuronal microRNAs. *Front Neurosci.* 2012;6:156. <https://doi.org/10.3389/fnins.2012.00156>.
  66. Uchida S, Hara K, Kobayashi A, Funato H, Hobara T, Otsuki K, et al. Early life stress enhances behavioral vulnerability to stress through the activation of REST4-mediated gene transcription in the medial prefrontal cortex of rodents. *J Neurosci.* 2010;30:15007–18. <https://doi.org/10.1523/JNEUROSCI.1436-10.2010>.
  67. Sigal JJ, DiNicola VF, Buonvino M. Grandchildren of survivors: can negative effects of prolonged exposure to excessive stress be observed two generations later? *Can J Psychiatry.* 1988;33:207–12. <https://doi.org/10.1177/070674378803300309>.
  68. Zamenhof S, van Marthens E, Grauel L. DNA (cell number) in neonatal brain: second generation (F2) alteration by maternal (F0) dietary protein restriction. *Science.* 1971;172: 850–1. <https://doi.org/10.1126/science.172.3985.850>.
  69. Nolan CJ, Damm P, Prentki M. Type 2 diabetes across generations: from pathophysiology to prevention and management. *Lancet.* 2011;378:169–81. [https://doi.org/10.1016/S0140-6736\(11\)60614-4](https://doi.org/10.1016/S0140-6736(11)60614-4).

70. Heynen JP, Paxman EJ, Sanghavi P, McCreary JK, Montina T, Metz GAS. Trans- and Multigenerational Maternal Social Isolation Stress Programs the Blood Plasma Metabolome in the F3 Generation. *Metabolites*. 2022;12. <https://doi.org/10.3390/metabo12070572>.
71. Lopes NA, Ambeskovic M, King SE, Faraji J, Soltanpour N, Falkenberg EA et al. Environmental Enrichment Promotes Transgenerational Programming of Uterine Inflammatory and Stress Markers Comparable to Gestational Chronic Variable Stress. *Int J Mol Sci.* 2023;24. <https://doi.org/10.3390/ijms24043734>.

## ACKNOWLEDGEMENTS

We thank Mr. Zhengrong Xia for technical assistance with the EM. This work was supported by National Natural Science Foundation of China (82304466), grants from the China Postdoctoral Science Foundation (2023T160070 and 2023M740372), Postdoctoral research funding from Changzhou Medical Center, Nanjing Medical University (CZKYCMCP202302), and Postgraduate Research & Practice Innovation Program of Jiangsu Province (JX10114060).

## AUTHOR CONTRIBUTIONS

YZ and MX designed the experiments. SC, SD and YP performed most of the experiments and analysis, YJ, PS, YL, CM, YW, ZW, TW and YZ did the behavioral experiment. The manuscript was written by MX and YZ. All authors discussed results, made figures, and edited the manuscript.

## COMPETING INTERESTS

The authors declare no competing interests.

## ADDITIONAL INFORMATION

**Supplementary information** The online version contains supplementary material available at <https://doi.org/10.1038/s41398-024-03109-1>.

**Correspondence** and requests for materials should be addressed to Yanli Zhang.

**Reprints and permission information** is available at <http://www.nature.com/reprints>

**Publisher's note** Springer Nature remains neutral with regard to jurisdictional claims in published maps and institutional affiliations.



**Open Access** This article is licensed under a Creative Commons Attribution-NonCommercial-NoDerivatives 4.0 International License, which permits any non-commercial use, sharing, distribution and reproduction in any medium or format, as long as you give appropriate credit to the original author(s) and the source, provide a link to the Creative Commons licence, and indicate if you modified the licensed material. You do not have permission under this licence to share adapted material derived from this article or parts of it. The images or other third party material in this article are included in the article's Creative Commons licence, unless indicated otherwise in a credit line to the material. If material is not included in the article's Creative Commons licence and your intended use is not permitted by statutory regulation or exceeds the permitted use, you will need to obtain permission directly from the copyright holder. To view a copy of this licence, visit <http://creativecommons.org/licenses/by-nc-nd/4.0/>.

© The Author(s) 2024